

Thermally tunable quadruple Vernier racetrack resonators

Robert Boeck,* Lukas Chrostowski, and Nicolas A. F. Jaeger

Department of Electrical and Computer Engineering, University of British Columbia, 2332 Main Mall,
Vancouver, BC V6T 1Z4, Canada

*Corresponding author: rboeck@ieee.org

Received March 18, 2013; revised May 22, 2013; accepted May 31, 2013;
posted June 10, 2013 (Doc. ID 187113); published July 9, 2013

The spectral responses of series-coupled racetrack resonators exhibiting the Vernier effect have many attractive features as compared to the spectral responses of identical series-coupled racetrack resonators, such as free spectral range (FSR) extension and enhanced wavelength tunability. Here we present experimental results of a thermally tunable quadruple series-coupled silicon racetrack resonator exhibiting the Vernier effect. We thermally tune two of the four racetrack resonators to enable discrete switching of the major peak by 15.54 nm. Also, our device has an interstitial peak suppression of 35.4 dB, a 3 dB bandwidth of 0.45 nm, and an extended FSR of 37.66 nm. © 2013 Optical Society of America

OCIS codes: (230.4555) Coupled resonators; (130.7408) Wavelength filtering devices; (250.5300) Photonic integrated circuits.

<http://dx.doi.org/10.1364/OL.38.002440>

Identical series-coupled ring resonators [1,2] have been fabricated in which each resonator has been thermally tuned. Thermal tuning is desirable because its effect on the effective index is large [3] and there is no excess loss versus current [4]. An increase in temperature tends to shift the resonant wavelength by approximately 0.07 nm/°C; therefore, to tune the resonant wavelength by the span of the C band (35.09 nm) would require a temperature change of several hundred degrees Celsius. Fortunately, the Vernier effect enables one to significantly enhance the resonant wavelength switching range as compared to the range available when using identical ring resonators [5]. Thermally tunable series [6,7] and cascaded [5,8] coupled ring resonator filters exhibiting the Vernier effect have been achieved previously. However, these devices show unacceptable spectral characteristics for typical dense wavelength-division multiplexing applications, such as low interstitial peak suppression (IPS) [5,6], small extension of the free spectral range (FSR) [6,7], and no extension of the FSR in the through port [5,8], and many do not use the silicon-on-insulator (SOI) platform [7,8]. Our previous results using double-racetrack resonators showed an IPS of 25.5 dB and a 3 dB bandwidth (BW) of 0.09 nm [9]; however, it is desirable to have larger IPSs and BWs. Previously, it has been theoretically shown that more than two serially coupled ring resonators are needed to achieve sufficient IPS [10–13] while maintaining a large enough BW. Here we experimentally demonstrate the first thermally tunable quadruple series-coupled Vernier racetrack resonator using SOI strip waveguides. We shift the major peak by 15.54 nm by heating two of the four racetrack resonators [resonators c and d in Fig. 1(a)].

For the modeling and analysis of our quadruple Vernier racetrack resonator, we have used SOI strip waveguides with heights of 220 nm and widths of 502 nm, as well as a top SiO₂ cladding. The Si refractive index is wavelength dependent and can be fitted to experimental data by using a Lorentz model [14]. Since the wavelength dependency of the refractive index of SiO₂ is minimal, we have assumed a constant refractive index of 1.4435. Also, we have used 2.4 dB/cm propagation loss in our modeling.

This is consistent with the value of 2.35 ± 0.33 dB/cm recently reported by [15] for SOI strip waveguides with top SiO₂ claddings. The schematic of the quadruple Vernier racetrack resonator is shown in Fig. 1(a), which has an asymmetric arrangement of resonators as described in [10–12,16]. The fabricated device is shown in Fig. 1(b).

$L_{a,b,c,d}$ are the total lengths of the racetrack resonators, κ_1 and κ_5 are the symmetric (real) point field coupling factors to the bus waveguides, $\kappa_{2,3,4}$ are the inter-ring symmetric (real) point field coupling factors, and $t_{1,2,3,4,5}$ are the respective (real) point field transmission factors. The derivations of the transfer functions can be found in [13,16]. The following simulations assume that $L_a = L_b = 2\pi r + 2L_x$ (where $r = 5 \mu\text{m}$ and $L_x = 7 \mu\text{m}$), $L_c = L_d = (4/3)L_a = 2\pi r + 2L_x + 2L$ (where $L = 7.569 \mu\text{m}$), $\kappa_1 = \kappa_5$, $\kappa_2 = \kappa_4$, $t_1 = t_5$, and $t_2 = t_4$. The effective index and field coupling and transmission factors are wavelength dependent and were determined using MODE Solutions software by Lumerical Solutions, Inc. The field coupling and transmission factors were calculated by determining the even and odd effective indices. At the major resonance wavelength (1545.96 nm), the effective index for a single waveguide is 2.4509, and its slope is -0.0011 nm^{-1} . The gap distances g_1, g_2, g_3, g_4 , and g_5 were chosen to be

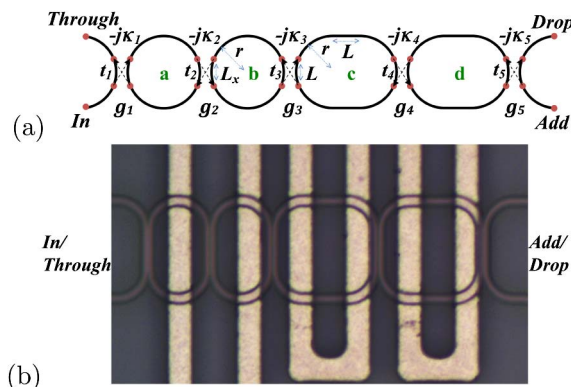


Fig. 1. (a) Schematic of the quadruple Vernier racetrack resonator and (b) the fabricated device.

148, 348, 388, 348, and 148 nm, respectively. At the major resonance wavelength, their respective field coupling factors (and slopes) are 0.4392 (0.0016 nm⁻¹), 0.0766 (0.0005 nm⁻¹), 0.0542 (0.0003 nm⁻¹), 0.0766 (0.0005 nm⁻¹), and 0.4392 (0.0016 nm⁻¹). We designed our device to have an express channel isolation, EC_i , greater than or equal to 25 dB [17] for a clear window of 0.1 nm at a center wavelength of 1545.94 nm and a channel spacing of 0.8 nm, as shown in Fig. 2(b), whereas our previous device had an EC_i of 11.1 dB for a clear window of 0.048 nm [16]. Also, minimal notches within the passband of the through port and a large IPS are required, as shown in Fig. 2(a). The 3 dB BW, IPS (defined as difference between the major peak intensity and the largest minor peak intensity), FSR, and EC_i are 0.34 nm, 41.0 dB, 36.93 nm, and 25.7 dB, respectively.

The device fabricated consisted of multiple e-beam lithography [18] and Cl₂ etch steps (to define the strip waveguides and shallow etch grating couplers), a 2 μm oxide deposition, followed by a 300 nm deposition of Al for the electrodes and metal heaters (5 μm wide) above the waveguides. Figures 3(a) and 3(b) show the experimental through port and drop port responses of the device when no voltage is applied. The FSR (37.09 nm) is larger than the span of the C band, the IPS is 26.6 dB, and the 3 dB BW is 0.24 nm. It is also clear that the through port response shows suppression of the resonances within the passband. The minimum insertion loss (defined as the maximum transmission at the through port) of the device is approximately 12 dB, which is due mainly to the grating coupler loss (typically measured to be 10–12 dB), whereas other loss mechanisms are minimal, such as mode-mismatch loss at the interfaces between straight sections and 90° bends of the racetrack resonators, which, based on our simulation results, is approximately 0.008 dB per interface. Also, one can

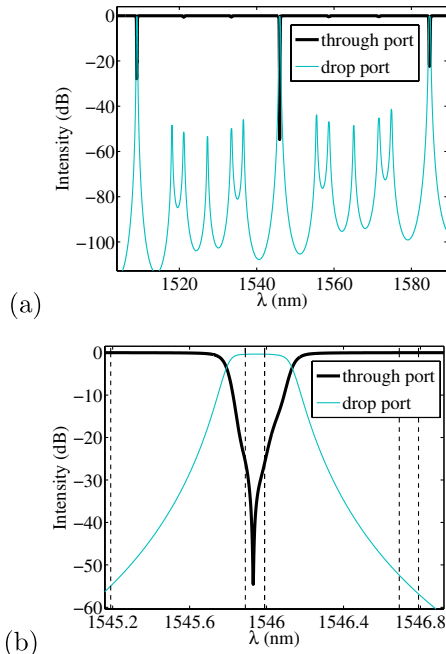


Fig. 2. (a) Theoretical through port and drop port spectra and (b) a major peak in the drop port response and a major notch in the through port response.

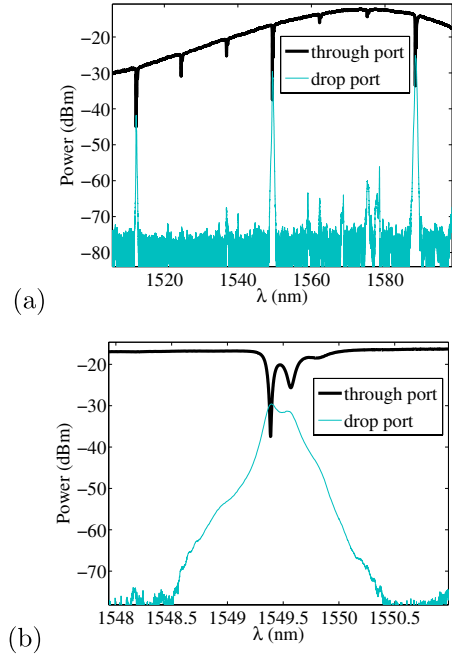


Fig. 3. (a) Experimental through port and drop port spectra and (b) a major peak of the drop port response and a major notch of the through port response.

clearly see that the major peak is much lower than the through port transmission and that the major notch shows worse performance as compared to the theory, which are likely due to fabrication variations and coupling-induced frequency shifts, which can be corrected for by finely tuning each ring resonator [1]. However, here we have focused on the discrete wavelength tunability of our device (continuous tuning is possible as described in [5]). We applied the same voltage to racetrack resonators c and d to enable the Vernier effect switching mechanism. Figure 4(a) shows the theoretical results when the temperature difference between resonators a and b, as compared to the temperature of resonators c and d, is increased from 0°C to 46°C ($dn/dT = 1.86 \times 10^{-4} \text{C}^{-1}$ [19]). We can clearly see the discrete switching of the major peak across a wavelength span of 12.70 nm, which corresponds to the FSR of a single racetrack resonator with the dimensions of one of our small resonators (i.e., resonator a or b). If we changed the temperatures of all of the racetrack resonators at the same time by 46°C, the major peak would shift by only 3.17 nm. Thus, we can see one of the benefits of using the Vernier effect to tune the resonant wavelength. Figure 4(b) shows the experimental results in which we varied the voltage applied to the heaters on top of both racetrack resonators c and d from 0 to 10.5 V. The major peak shifts discretely by 15.54 nm. When 10.5 V is applied, the major peak has an IPS of 33.9 dB, a 3 dB BW of 0.45 nm, and an FSR of 37.66 nm. If we define the IPS for a clear window of 0.1 and 0.8 nm channel spacing, the IPS is 35.4 dB. Except for a 2.84 nm increase in the resonant shift, which is possibly due to thermal cross talk between the racetrack resonators [5] (resonators a and b are likely also being heated), the experimental Vernier switching mechanism seen here is in agreement with the theoretical results.

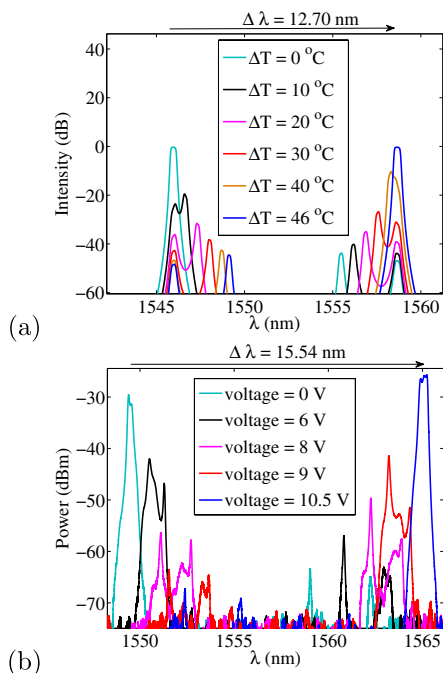


Fig. 4. (a) Theoretical drop port spectral responses for various temperature changes applied to racetrack resonators c and d and (b) experimental drop port spectral responses for various changes in the voltage applied to the heaters on top of racetrack resonators c and d.

In summary, we have demonstrated a thermally tunable quadruple Vernier racetrack resonator. This device has an IPS of 35.4 dB, a 3 dB BW of 0.45 nm, and an extended FSR of 37.66 nm when 10.5 V is applied to the heaters on top of the two larger racetrack resonators. We were also able to shift the major peak by 15.54 nm.

We acknowledge the Natural Sciences and Engineering Research Council of Canada and Lumerical Solutions, Inc., for their support of this work. We thank Yun Wang, Jonas Flueckiger, and Charlie Lin for their technical assistance and Alina Kulpa for the microscope image. Part of this work was conducted at the University of Washington Microfabrication Facility, a member of the NSF National Nanotechnology Infrastructure Network. Also, we thank Edgar Huante-Ceron and Andy Knights at McMaster University for the metallization.

References and Note

1. P. Prabhathan, V. M. Murukeshan, and J. Zhang, *Opt. Eng.* **51**, 044604 (2012).
2. M. A. Popovic, T. Barwicz, M. S. Dahlem, F. Gan, C. W. Holzwarth, P. T. Rakich, H. I. Smith, E. P. Ippen, and F. X. Krtner, in *2007 33rd European Conference and Exhibition of Optical Communication (ECOC)* (IEEE, 2007), pp. 1–2.
3. N. Sherwood-Droz, H. Wang, L. Chen, B. G. Lee, A. Biberman, K. Bergman, and M. Lipson, *Opt. Express* **16**, 15915 (2008).
4. M. Geng, L. Jia, L. Zhang, L. Yang, P. Chen, T. Wang, and Y. Liu, *Opt. Express* **17**, 5502 (2009).
5. P. Prabhathan, Z. Jing, V. M. Murukeshan, Z. Huijuan, and C. Shiyi, *IEEE Photon. Technol. Lett.* **24**, 152 (2012).
6. W. S. Fegadolli, G. Vargas, X. Wang, F. Valini, L. A. M. Barea, J. E. B. Oliveira, N. Frateschi, A. Scherer, V. R. Almeida, and R. R. Panepucci, *Opt. Express* **20**, 14722 (2012).
7. Y. Goebuchi, T. Kato, and Y. Kokubun, in *The 18th Annual Meeting of the IEEE Lasers and Electro-Optics Society, 2005 (LEOS 2005)* (IEEE, 2005), pp. 734–735.
8. S. T. Chu, B. E. Little, V. Van, J. V. Hryniewicz, P. P. Absil, F. G. Johnson, D. Gill, O. King, F. Seiferth, M. Trakalo, and J. Shanton, in *Optical Fiber Communication Conference, Technical Digest (CD)* (Optical Society of America, 2004), paper PD9.
9. R. Boeck, J. Flueckiger, H. Yun, L. Chrostowski, and N. A. F. Jaeger, *Opt. Lett.* **37**, 5199 (2012).
10. Y. Goebuchi, T. Kato, and Y. Kokubun, *Jpn. J. Appl. Phys.* **45**, 5769 (2006).
11. D. Zhang, Y. Huang, X. Ren, X. Duan, B. Shen, Q. Wang, X. Zhang, and S. Cai, *Proc. SPIE* **8555**, 85550U (2012).
12. O. Schwelb and I. Frigyes, *Microw. Opt. Technol. Lett.* **39**, 257 (2003).
13. S. Dey and S. Mandal, *Opt. Commun.* **285**, 439 (2012).
14. L. Chrostowski and M. Hochberg, *Silicon Photonics Design* (Lulu, 2013).
15. R. Ding, T. Baehr-Jones, T. Pinguet, J. Li, N. C. Harris, M. Streshinsky, L. He, A. Novack, E.-J. Lim, T.-Y. Liow, H.-G. Teo, G.-Q. Lo, and M. Hochberg, in *Optical Fiber Communication Conference, OSA Technical Digest* (Optical Society of America, 2012), paper OM2E.6.
16. R. Boeck, J. Flueckiger, L. Chrostowski, and N. A. F. Jaeger, *Opt. Express* **21**, 9103 (2013).
17. Alliance Fiber Optic Products, Inc.
18. R. J. Bojko, J. Li, L. He, T. Baehr-Jones, M. Hochberg, and Y. Aida, *J. Vac. Sci. Technol.* **B 29**, 06F309 (2011).
19. P. Dong, W. Qian, H. Liang, R. Shafiha, N. N. Feng, D. Feng, X. Zheng, A. V. Krishnamoorthy, and M. Asghari, *Opt. Express* **18**, 9852 (2010).